International Journal of Signal Processing, Image Processing and Pattern Recognition
Vol.9, No.2 (2016), pp.393-404
http://dx.doi.org/10.14257/ijsip.2016.9.2.33

Combination of LLT Model and TV Model for Image Denoising

Fengqi Zhou[1], Yu Xiao[1], Zhigang Yan[2], Fenlin Yang[3]

[1]*School of Basic Science, East China Jiaotong University, Nanchang, 330013, China*

[2]*Accounting School, Jiangxi University of Finance and Economics, Nanchang, 330013, China*

[3]*College of Mathematics and Statistics, Jishou University, Jishou, 416000, China*

yuyugongwu@163.com

Abstract

Developing a variational model that is capable of restoring both smooth (no edges) and non-smooth (with edges) images is still a valid challenge at the image processing. In this paper, we present two methods for image denoising problems based on the use of the LLT model (see [14]) and TV model (see [20]). The idea of our methods is, add the texture which is separated from the cartoon and noisy, back to the original noisy image or the texture plus noisy part, and the sum then processed. In order to obtain the texture, we first separate texture plus noise from cartoon by LLT model, and then use TV model to remove some noisy from texture. Numerical experiments show our method is able to maintain some important information such as small details in the image, and at the same time to get a better visualization.

Keywords: *Image denoising, staircasing effect, iterated regularization, cartoon and texture, image decompose.*

1. Introduction

A “quality" image is essential for further image processing tasks such as edge detection, pattern recognition, and object tracking, etc. Image denoising is one of the tasks to extract a “quality" image u from the noisy image f by the degradation model

$$f(x,y) = u(x,y) + \eta(x,y), \quad (x,y) \in \Omega, \tag{1}$$

where Ω is a bounded convex region of P^2 and η is an additive noise term.

Many different variational techniques are proposed to obtain an estimate of u (see [25], [14], [16], [10] for details). The total variation (TV) model by Rudin, Osher and Fatemi in [20] is an effective and well known method, which consists of solving the following problem:

$$\min_u \ \alpha \int_\Omega |\nabla u| dxdy + \frac{1}{2}\Pi u - f\Pi^2. \tag{2}$$

Here $|\cdot|$ is the Euclidean norm in P^2, $\Pi\cdot\Pi$ is the norm in $\mathbf{L}^2(\Omega)$, α is a positive parameter controlling the trade-off between goodness of fit-to-the-data and variability in u. The corresponding Euler Lagrange partial differential equation (PDE) is

$$g(u) = -\alpha\nabla\cdot\left(\frac{\nabla u}{\sqrt{|\nabla u|^2 + \beta}}\right) + (u - f) = 0, \tag{3}$$

with homogeneous Neumann boundary condition $\partial u/\partial\vec{n} = 0$. Here β is a small positive parameter, and $\vec{n}$ is the normal vector of boundary. Equation (3) is second order, and there are many fast and efficient methods (see [20, 23, 7, 17, 6, 9, 18]). Furthermore, this model can preserve shape edges and boundaries with a high quality recovery. But for

ISSN: 2005-4254 IJSIP

images without edges (jumps), the solution to this model has the undesirable staircasing effect. In order to remedy the staircase effects, some effort has been made ([14, 15, 17, 19, 4, 21, 8, 11, 27, 12, 3]). In [14], Lysaker, Lundervold and Tai (LLT) proposed a second order functional minimization by the following formula:

$$\min_u \ \alpha \int_\Omega | D^2 u | dxdy \ + \frac{1}{2} \Pi u - f \Pi^2, \tag{4}$$

where $| D^2 u | = \sqrt{u_{xx}^2 + u_{xy}^2 + u_{yx}^2 + u_{yy}^2}$. The corresponding Euler Lagrange PDE for (4) is

$$g_2(u) = \alpha [(\frac{u_{xx}}{| D^2 u |_\beta})_{xx} + (\frac{u_{xy}}{| D^2 u |_\beta})_{yx} + (\frac{u_{yx}}{| D^2 u |_\beta})_{xy} + (\frac{u_{yy}}{| D^2 u |_\beta})_{yy}] + (u - f) = 0, \tag{5}$$

where $| D^2 u |_\beta = \sqrt{u_{xx}^2 + u_{xy}^2 + u_{yx}^2 + u_{yy}^2 + \beta}$ $(\beta > 0)$. The use of fourth order derivatives damps out high frequency components of the image, so (5) can recover smoother surfaces and produce better approximation to the nature image. However such models cannot preserve sharp features such as jumps; it is a challenge for a single model to restore both smooth and non-smooth images.

Zhu and Chan [27] try to find a piecewise smooth surface to approximate the image surface by incorporating the corresponding geometric quantities – mean curvature into the processing of denoising

$$\min_u \ \{ J(u) = \alpha \int_\Omega \Phi(\kappa) dxdy \ + \frac{1}{2} \Pi u - f \Pi^2 \}. \tag{6}$$

Here κ is the mean curvature of the image which is defined by

$$\kappa = \nabla \cdot \frac{\nabla u}{| \nabla u |}, \tag{7}$$

and the function Φ is defined either as $\Phi(\kappa) = | \kappa |$, $\Phi(\kappa) = \kappa^2$ or a combination of both.

Although the mean curvature model can avoid the staircase effect, the fourth order partial differential equations (PDE) arising from (6) is

$$g_\beta(u) = \alpha \nabla \cdot (\frac{1}{| \nabla u |_\beta} (I_2 - \frac{\nabla u \nabla u^T}{| \nabla u |_\beta^2}) \nabla \Phi'(\kappa_\beta(u))) + (u - f) = 0, \tag{8}$$
$$\nabla u \cdot \vec{n} = 0 \qquad (x, y) \in \partial\Omega,$$

where $I_2 \in P^{2\times 2}$ is the identity matrix. The construction of stable numerical schemes for the above PDE is very difficult due to high nonlinearity and stiffness. In [26], Yang, Chen and Yu used a homotopy idea to devise a feasible method. But an equation of type (8) has to be solved several times.

In recent years, among others, researchers have turned to the combination TV model and LLT model (see [16, 10]). Lysaker and Tai [16] suggested a convex combination of the respective two solutions from (3) and (5). Specifically, with $w^0 = f$, a new iteration w^{k+1} is generated by the convex combination

$$w^{k+1} = \theta^k v^{k+1} + (1 - \theta^k) u^{k+1} \qquad k = 0,1,2 \ \cdots, \tag{9}$$

where v^{k+1} and u^{k+1} are respectively obtained by the k th time marching iteration of TV model and LLT model with w^k as their old iteration. Here the parameter θ^k which is applied to control the combination depends on ∇w^k. There are some other combination methods, such as the TGV method by Bredies K., Kunisch K. and T. Pock ([2]), a weighted H1 seminorm regularization method by Lin and Yang ([13]) and some methods included in [1] by P. Blomgren, T. Chan, and P. Mulet .

The above convex combination solution (9) reduces to the TV solution in regions where $| \nabla u |$ is large (near edges) or to the LLT solution where $| \nabla u |$ is 0 (flat regions).

It would be better to use the TV solution when $|\nabla u| \approx 0$, and also one may wish to solve a single PDE (from a combined optimization) instead of solving two separate PDEs. This is the idea taken up in [10] by Chang, Tai and Xing who proposed a new combination of the TV model and the LLT model in the form

$$\min_u \{\alpha(\int_\Omega \theta |\nabla u| dxdy + \int_\Omega (1-\theta)|D^2 u| dxdy) + \frac{1}{2}\|u - f\|^2\}, \quad (10)$$

where θ is the variable parameter.

Numerical results show these algorithms can inherit the advantages of the TV model and the LLT model, and avoid the disadvantages of both models in some degree. However, as far as the restored smooth parts are concerned, theirs are not as well as that for the LLT model, and the restored edges are not as well as that for TV model.

In this paper, we intend to restore effectively both smooth images (with no clear jumps) and blocky images (of piecewise constant intensities) by the iterated regularization of LLT model and TV model. Note that the advantages of the LLT model and the TV model, our procedure would use these two models to decompose the original noisy image f into three components, including the piecewise-smooth component u, the oscillatory component v and the third represents noisy η, and add v back to the original noisy image f or $f-u$, the sum then proceed.

The rest of this paper is organized as follows. In Section 2, we first review the iterated total variation refinement. In Section 3, we describe our method in detail. Finally, numerical results of the proposed algorithms on several tests are given in Section 4.

2. Iterated regularization method

The ideal result of the denoising method would be decompose f into the true signal u and the additive noise η without any signal. In practice, this is not fully attainable. Take the TV model for example, the removed noise is treated as an error, some details, such as texture will be swept as an error. Some effort has been made to extract more meaningful signals from the noise part η (see [19, 22]). In [19], Osher, Martin, et al. proposed an iterated regularization procedure to preserve some details from the removed noise part. They added the removed noise computed by TV model back to the original noise image f, and the sum then processed by the total variation method. This regularization procedure is repeated as follows:

Step 1. Set $\eta_0 = 0,\ k = 0$.

Step 2. Compute u_{k+1} as a minimizer of the modified TV model,

$$u_{k+1} = \arg\min_u \{\alpha \int_\Omega |\nabla u| dxdy + \frac{1}{2}\|f + \eta_k - u\|^2\}.$$

Step 3. Update

$$\eta_{k+1} = \eta_k + f - u_{k+1},$$

and set $k := k+1$, then return to step 2.

It is enough to proceed iteratively until the result gets noisier or the distance $\|u_k - u\|^2$ gets smaller than σ^2, where u is the original image and σ is the standard deviation of the added noise.

3. Iterated regularization methods based on LLT model and TV model

In the ideal denoising case, ideal methods would be restoring effectively both blocky images (of piecewise constant intensities) and smooth images (with no clear jumps). As in

the above discussion, we know a smooth primal sketch u can be obtained by the LLT model, and the removed part $f - u$ is texture plus noise, which is also a noisy image, and can be denoised by the TV model and the mean curvature model.

Here we consider a decomposition $f = u + v + \eta$, where u represents piecewise-smooth (cartoon or structure) component of f, v represents the oscillatory components of f, i.e. texture, and η represents residual (noise). The idea of our method is, add the texture v back to the original noisy image f or the remove part $f - u$, and the sum is processed. In order to obtain the texture v, we first separate texture plus noise from cartoon by LLT model, and then use TV model to remove some noisy from $f - u$. In this section, we will introduce two algorithms for image denoising.

3.1. Algorithm 1

Our algorithm 1 is constructed by adding the texture v back to the original noisy image f, and obtianing the sum $f + v$ by the LLT model. The details of our algorithm are given in the following

1. First, separate the cartoon u from texture plus noise by the original LLT model

$$u = \arg \min_{u} \{\alpha_0 \int_{\Omega} | D^2 u | dxdy + \frac{1}{2} \| u - f \|^2 \},$$

   and obtain the texture plus noise $f - u$.
2. Second, remove some noisy from $f - u$ by the TV model

$$v = \arg \min_{v} \{\alpha_1 \int_{\Omega} | \nabla v | dxdy + \frac{1}{2} \| v - (f - u) \|^2 \},$$

   and obtain the texture v (maybe plus little noisy).
3. Add the texture v back to the original noisy image f.
4. Finally, the sum $f + v$ is proceed by the LLT model

$$u = \arg \min_{u} \{\alpha_0 \int_{\Omega} | D^2 u | dxdy + \frac{1}{2} \| u - (f + v) \|^2 \}.$$

   and obtain the recovered image u.

Here α_0 and α_1 are regularization parameters.

3.2. Algorithm 2

Clearly, the noise $f - u$ computed by the LLT model contains some details, such as texture, and we can treat this part as the noisy image. Since the cartoon is separated, we consider use the improved iterated total variation procedure to extract some more signals from $f - u$. The details of our algorithm are given in the following

1. First, decompose the original image f into the cartoon u and the texture plus noise by the LLT model

$$u = \arg \min_{u} \{\alpha_0 \int_{\Omega} | D^2 u | dxdy + \frac{1}{2} \| u - f \|^2 \},$$

   and obtain the texture plus noise $f - u$.
2. Second, remove some noisy from $f - u$ by the TV model

$$v_0 = \arg \min_{v} \{\alpha_1 \int_{\Omega} | \nabla v | dxdy + \frac{1}{2} \| v - (f - u) \|^2 \},$$

   and obtain the texture v_0 (maybe plus little noisy).
3. Add the texture v_0 back to $f - u$.

4. The sum $f - u + v_0$ is proceed by the TV model

$$v = \arg \min_{v} \{\alpha_2 \int_{\Omega} |\nabla v| dxdy + \frac{1}{2} \Pi v - (f - u + v_0) \Pi^2 \}.$$

5. Finally, add the texture v back to the cartoon u, then $u = u + v$ is the recovered image.

4. Numerical experiments and discussions

In this section, we present some of the results by comparing our algorithms with some other classical denoising methods. We use the signal to noise ratio (SNR), and the difference between a digital image and its denoised version to measure the quality of the restored images. They are defined by

$$SNR = 10 \log_{10} \frac{\sum_{i=1}^{n} \sum_{j=1}^{n} u_{i,j}^2}{\sum_{i=1}^{n} \sum_{j=1}^{n} (u_{i,j} - \tilde{u}_{i,j})^2},$$

and

$$diff(\tilde{u}) = \tilde{u} - f,$$

where u and $\tilde{u}$ are the original image and the restored image, respectively.

4.1. Comparisons of our algorithms with the TV model and the LLT model

Below we compare our methods with the TV model and LLT model. Since the TV model does well in “blocky" images and LLT model works almost perfectly for smooth images, we choose the standard “Lena" image as the test image which is composed of flat subregions, subregions with a smooth change in intensity value and jumps. The original and noisy images are shown in Figure 1. From the restored results of Figure 2 and Figure 3, we see that the recovered images by the LLT model and our algorithms are visually better than the TV model, and images denoised by the TV model and our methods preserve the edges better than the LLT model.

To highlight our algorithms can restore effectively both smooth images (with no clear jumps) and blocky images (of piecewise constant intensities), we extract the flat subregions and the smooth subregions of the original, noisy and restored images of “Lena" (see Figures 4-7). It is remarkable that both the recovered flat subregions and the recovered smooth subregions by our algorithms are qualified as well as the TV model and the LLT model. We can also see the strengths and weakness about both TV model and LLT model.

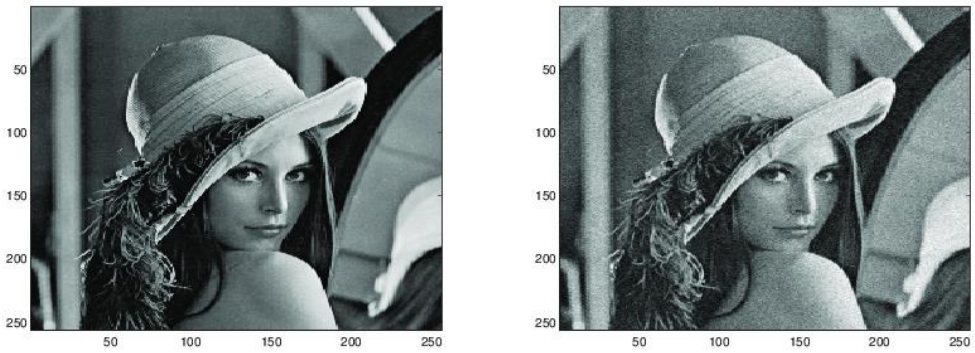

Figure 1. Left Plot: The original “Lena" image. Right Plot: Noisy image of “Lena" (SNR=20.97).

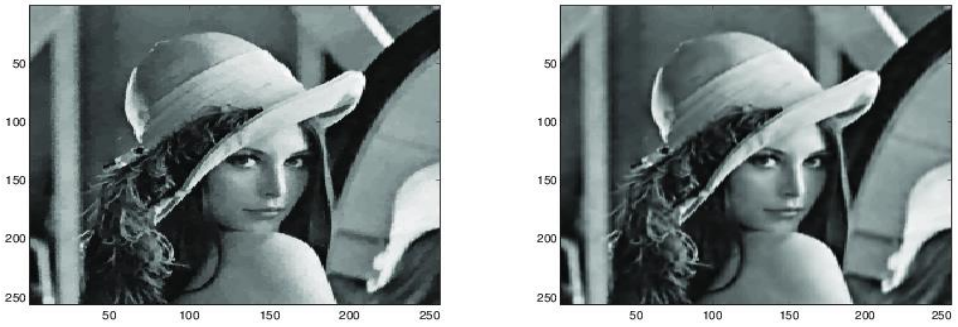

Figure 2. Left Plot: Image recovered by TV model with SNR=25.39. Right Plot: By LLT model with SNR=24.81

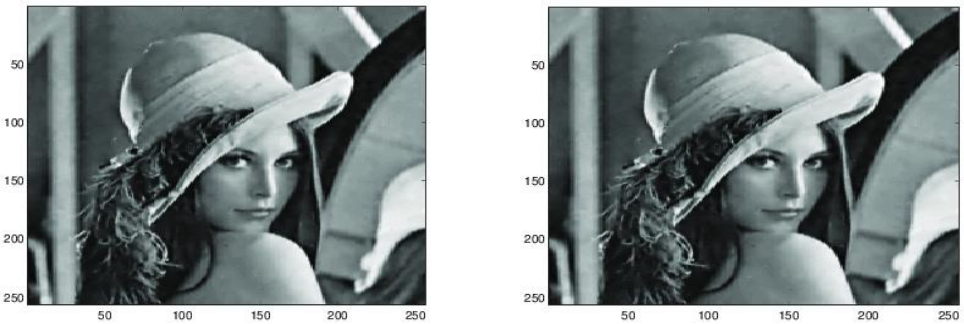

Figure 3. Left Plot: Image recovered by algorithm 1 with SNR=26.18. Right Plot: By algorithm 2 with SNR=26.19

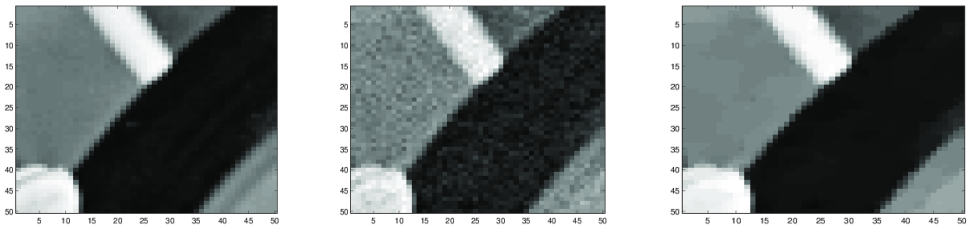

Figure 4. Left and Middle Plot: The flat subregions of original “Lena" image and noisy image. Right Plot: The subregion recovered by TV model

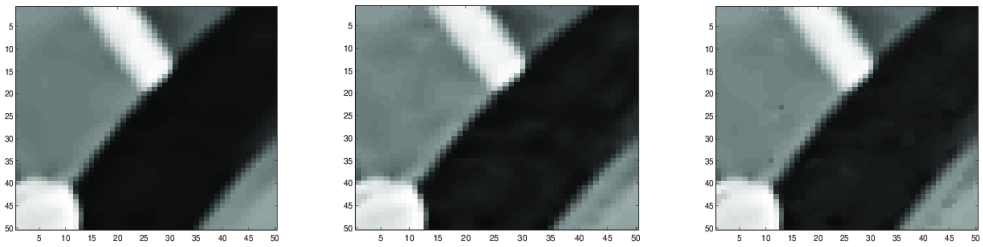

Figure 5. Left and Middle Plot: The flat subregions recovered by LLT model and algorithm 1. Right Plot: by algorithm 2

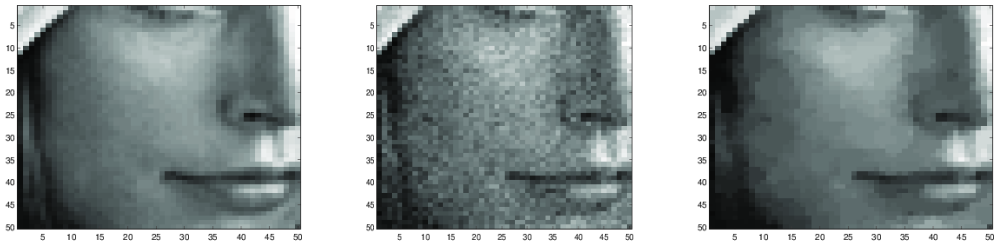

Figure 6. Left and Middle Plot: The smooth subregions of original "Lena" image and noisy image. Right Plot: The subregion recovered by TV model

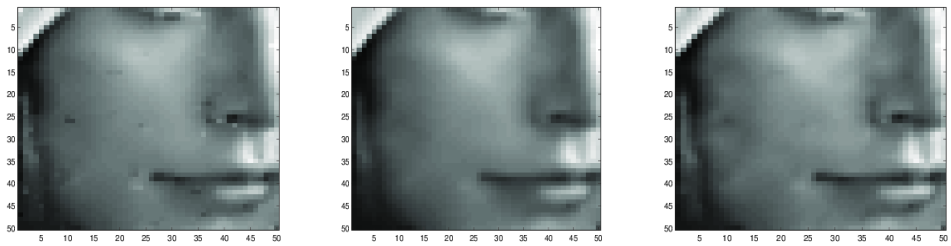

Figure 7. Left and Middle Plot: The smooth subregions recovered by LLT model and algorithm 1. Right Plot: by algorithm 2

4.2. Comparison of Algorithm 1 with the Mean Curvature Model

Our next test uses an image containing both a human face and some textures (see Figure 8). The challenge with this image is to maintain both texture details and smooth transitions in the human face during processing. As a high order model, Mean curvature model is known to yield satisfying results for restoring small details and enhancing the recovery of smooth subsurfaces contained in the image. In this section, we compare this method with algorithm 1. The difference images tell us that both methods can restore textures on the scarf in a proper way, but the background and human feature like a hand, shoulder, and face are visually better by our algorithm (see Figure 9 and 10).

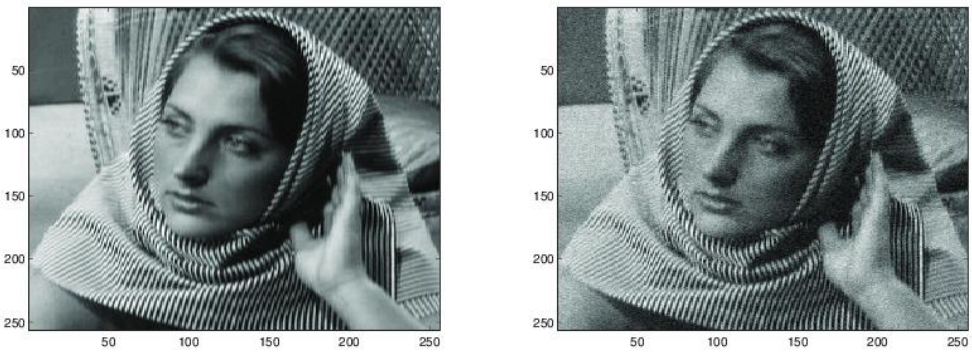

Figure 8. Left Plot: The original "barbara" image. Right Plot: Noisy image of "barbara" (SNR=22.04)

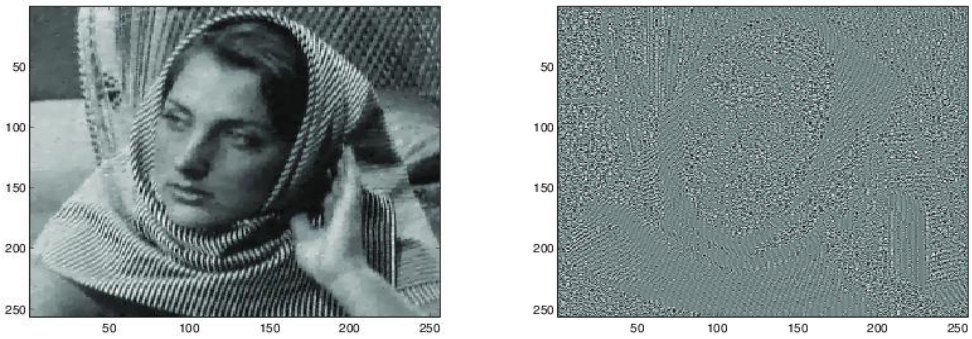

Figure 9. Left Plot: Image recovered by mean curvature model with SNR=24.89. Right Plot: The difference image

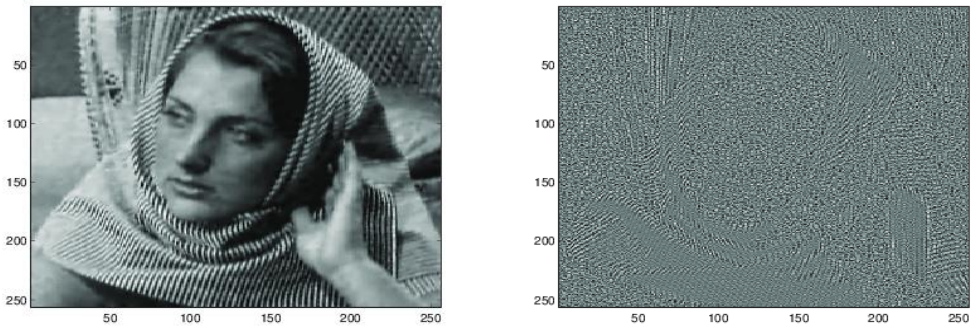

Figure 10. Left Plot: Image recovered by algorithm 1 with SNR=25.40. Right Plot: The difference image

4.3. Comparison of Algorithm 1 with the convex combination method

Image restoration combining total variation minimization and a second-order functional ([10]) can restore effectively both the blocky subregion (of piecewise constant intensities) and smooth subregion (with no clear jumps) of an image. The above two numerical examples show our method also inherit the advantages of the TV model and the LLT model. The third example concerns an "Aircraft" image, which is corrupted with zero mean Gaussian random noise (see Figure 11). Both the convex combination method ([10]) and our method obtain a good visualization, but the difference images tell us that our method works better on preserving small details (see Figures 12 -13).

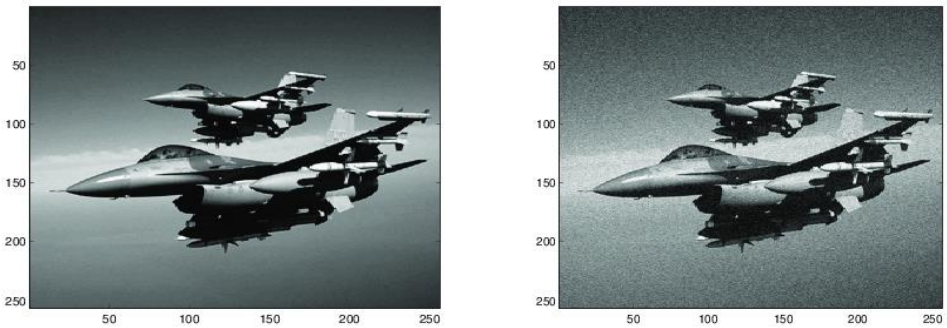

Figure 11. Left Plot: The original "Aircraft" image. Right Plot: Noisy image of "Aircraft" (SNR=21.76)

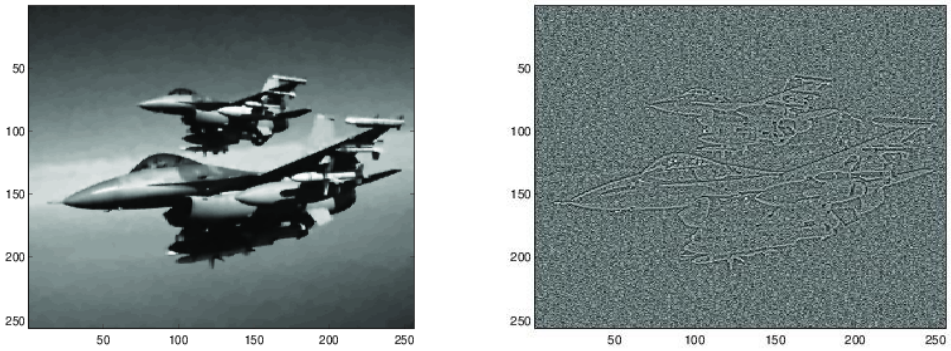

Figure 12. Left Plot: Image recovered by the convex combination method with SNR=26.69. Right Plot: The difference image

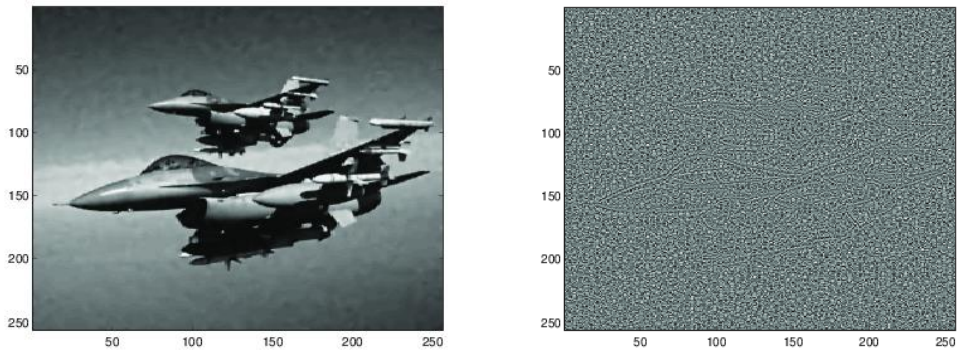

Figure 13. Left Plot: Image recovered by algorithm 1 with SNR=28.64. Right Plot: The difference image

4.4. Comparisons of Algorithm 1 with some other methods

The final example concerns a “Pepper" image which contains some smooth transitions (see Figure 11). The purpose of this test is to show our algorithm is qualified with maintaining the smooth transitions. Here we refer to some improved TV models such as the split bregman anisotropic and isotropic total variation denoising methods ([12]) and the spatially dependent parameter selection method ([3]), and high order models like the mean curvature model and TGV model. Numerical results (see Figures 15-17) show the visualization by the TGV method and our method are better, and the SNR obtained by our method is the highest of all.

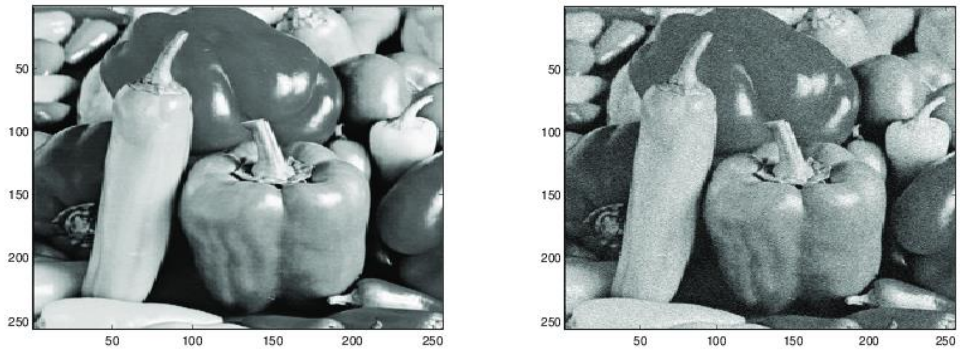

Figure 14. Left Plot: The original “Pepper" image. Right Plot: The noisy image

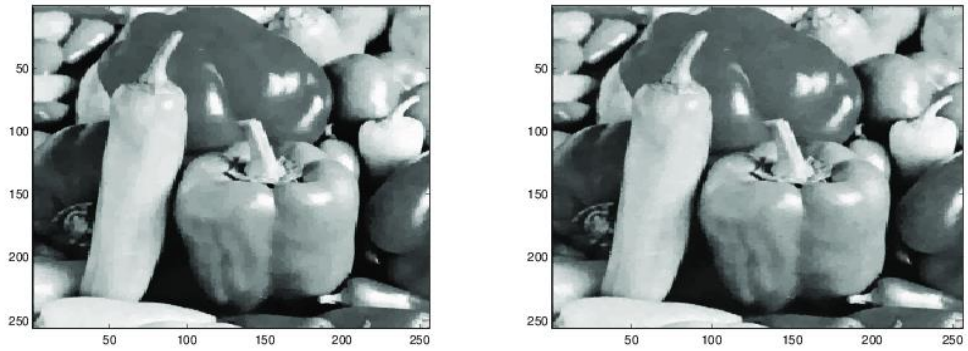

Figure 15. Left Plot: Image recovered by split Bregman anisotropic total variation denoising method with SNR=27.34. Right Plot: By split Bregman isotropic total variation denoising method with SNR=27.88

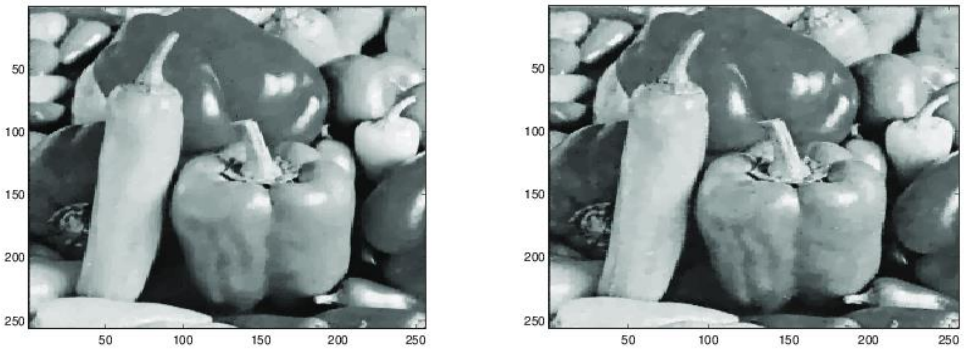

Figure 16. Left Plot: Image recovered by the spatially dependent parameter selection method for TV model with SNR=27.98. Right Plot: By mean curvature model with SNR=27.99

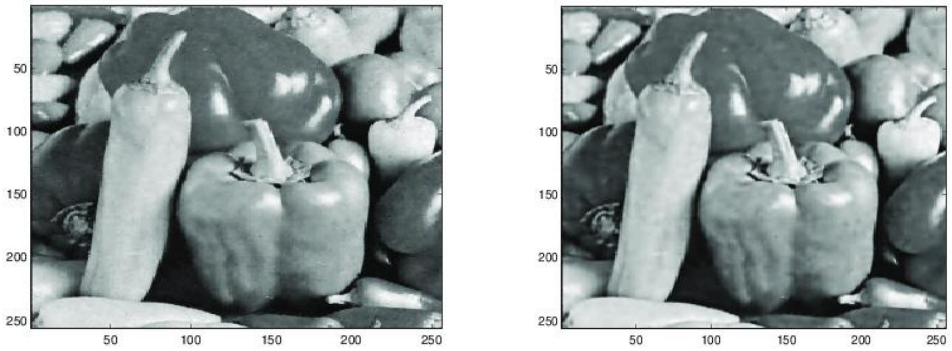

Figure 17. Left Plot: Image Recovered by the TGV method with SNR=27.90. Right Plot: By Algorithm 1 with SNR=28.54

4. Conclusions

Image denoising combining total variation minimization and a second-order functional can restore effectively both the blocky subregion (of piecewise constant intensities) and smooth subregion (with no clear jumps) of an image. In this paper, we proposed two new methods to inherit the advantages of the TV model and the LLT model. Our methods are

constructed by adding the texture which is separated from the cartoon and noisy back to the original image or the texture plus noisy part, and the sum then proceed. The procedure for getting the texture is simple. Firstly, we make full use of the advantages of the LLT model to separate the cartoon. Then, we try to remove some noisy from the remain part by the TV model. With these approaches, most of the texture plus less noisy are extracted. If we reject using the LLT model in the first step, other models which can separate a smooth cartoon is all right. Numerical experiments substantiate that our methods inherit the advantages of the TV model and the LLT model better than the convex combination methods.

Acknowledgments

This work was supported by the National Natural Science Foundation of China (11126172 and 11261019).

References

[1]. P. Blomgren, T. Chan, and P. Mulet, Total variation image restoration: Numerical methods and extentions, Proceeding of IEEE Int'1 Conference on Image Processing, 3**(1997)**, pp. 384-387.
[2]. K. Bredies, K. Kunisch and T. Pock, Total generalized variation, SIAM J. Imaging Sci., vol. 3, no. 3 **(2010)**, pp. 492-526.
[3]. K. Bredies, Y. Q. Dong and M. Hinternüller, Spatially dependent parameter selection in total generalized variation model for image restoration, International Journal of Computer Mathematics, vol. 90, no. 1, **(2013)**, pp. 109-123.
[4]. C. Brito-Loeza and K. Chen, Multigrid algorithm for high order denoising, SIAM J. Imaging Sciences, vol. 3, no. 3, **(2010)**, pp. 363-389.
[5]. A. Chambolle and P.-L. Lions, Image recovery via total variation minimization and related problems, Numer. Math., vol. 76, no. 2, **(1997)**, pp. 167-188.
[6]. A. Chambolle, An algorithm for total variation minimization and applications, J. Math. Imaging Vis., vol. 20, no. 1-2, **(2004)**, pp. 89-97.
[7]. T. F. Chan, G. H. Golub and P. Mulet, A nonlinear primal-dual method for total variation-based image restoration, SIAM J. Sci. Comput., vol. 20, no. 6, **(1999)**, pp. 1964-1977.
[8]. T. F. Chan, A. Marquina and P. Mulet, High-order total variation-based image restoration, SIAM J. Sci. Comput., vol. 22, no. 2, **(2000)**, pp. 503-516.
[9]. T. F. Chan and J. H. Shen, Image Processing and Analysis-Variational, PDE, Wavelet, And Stochastic Methods, SIAM, Philadelphia, **(2005)**.
[10]. Q. S. Chang, X. C. Tai and L. Xing, A compound algorithm of denoising using second-order and fourth-order partial differential equations, Numer. Math. Theor. Meth. Appl., vol. 2, no. 4, **(2009**), pp. 353-376.
[11]. S. Didas, B. Burgeth, A. Imiya and J. Weickert, Regularity and Scale-Space Properties of Fractional High Order Linear Filtering, Scale-Space and PDE Methods in Computer Vision, volume 3459 of Lecture Notes in Computer Science, Springer, Berlin, **(2005)**.
[12]. T. Goldstein and S. Osher, The split Bregman method for L1 regularized problems, SIAM Journal on Imaging Sciences, vol. 2, no. 2, **(2009)**, pp. 323-343.
[13]. F. R. Lin and S. W. Yang, A weighted H^1 seminorm regularization method for Fredholm integral equations, Int. J. Comput. Math., vol .91, no. 5, **(2014)**, pp. 1012-1029.
[14].M. Lysaker, A. Lundervold and X. C. Tai, Noise removal using fourth-order partial differential equation with applications to medical magnetic resonance images in space and time, IEEE Transactions on Image Processing, vol. 12, no. 12, **(2003)**, pp.1579-1590.
[15]. M. Lysaker, S. Osher and X. C. Tai, Noise removal using smoothed normals and surface fitting, IEEE Transactions on Image Processing, vol. 13, no. 10, **(2004)**, pp. 1345-1357.
[16]. M. Lysaker and X. C. Tai, Iterative image restoration combining total variation minimization and a second-order functional, Int. J. Comput. Vision, vol. 66, no. 1, **(2006)**, pp. 5-18.
[17]. A. Marquina and S. Osher, Explicit algorithms for a new time dependent model based on level set motion for nonlinear deblurring and noise removal, SIAM J. Sci. Comput., vol. 2, no. 2, **(2000)**, pp. 387-405.
[18]. S. Osher and R. Fedkiw, Level Set Methods and Dynamic Implicit Surfaces, Springer, New York, **(2003)**.
[19]. S. Osher, M. Burger, D. Goldfarb, Jinjun Xu and Wotao Yin, An iterative regularization method for total variation-based image restoration, Multiscale Modeling and Simulation, vol. 4, no. 2, **(2005)**, pp. 460-489.
[20]. Leonid I. Rudin, S. Osher and E. Fatemi, Nonlinear total variation based noise removal algorithms, Phys. D, vol. 60, no. 1-4, **(1992)**, pp. 259-268.

[21]. J. Savage and K. Chen, On multigrids for solving a class of improved total variation based staircasing reduction models, Springer-Verlag, Berlin, **(2007)**, pp. 69-94.
[22]. E. Tadmor, S. Nezzar, and L. Vese, A multiscale image representation using hierarchical (BV , L_2) decompositions, Multiscale Modeling and Simulation, vol. 2, no. 4, **(2004)**, pp. 554-579.
[23]. C. R. Vogel and M. E. Oman, Iterative methods for total variation denoising, SIAM J. Sci. Comput., vol. 17, no. 1, **(1996)**, pp. 227-238.
[24]. C. R. Vogel and M. E. Oman, Fast, robust total variation-based reconstruction of noisy, blurred images, IEEE Transactions on Image Processing, vol. 7, no. 6, **(1998)**, pp. 813-824.
[25]. C. R. Vogel, Computational Methods for Inverse Problems, SIAM, Philadelphia, **(2002)**.
[26]. F. L. Yang, K. Chen and B. Yu, Homotopy method for a mean curvature-based denoising model, Applied Numerical Mathematics, vol. 62, no. 3, **(2012)**, pp.185-200.
[27]. W. Zhu and T. F. Chan, Image denoising using mean curvature of image surface, SIAM J. Image Sci., vol. 5, no. 1, **(2012)**, pp. 1-32.

Authors

Fengqi Zhou she received her master degree in mathematical sciences, from Dalian university of technology (2005). She is currently a lecturer of east china jiaotong university. Her current research interests include neural network, image processing.

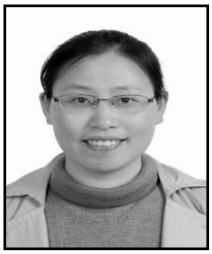

Yu Xiao she received her Ph.D. degree in mathematical sciences, from Dalian university of technology (2010). She is currently a lecturer of east china jiaotong university. Her current research interests include numerical optimization, data mining, image processing.

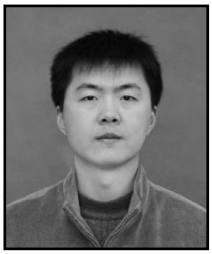

Zhigang Yan he received his Ph.D. degree in Dongbei University of finance and economics (2013). He is currently a lecturer of Jiangxi University of finance and economics. His current research interests include numerical optimization, data mining.

Fenlin Yang she received her Ph.D. degree in mathematical sciences, from Dalian university of technology (2012). She is currently a lecturer of Jishou university. Her current research interests include numerical optimization, image processing.

